Article

Current Biology

CPG2 Recruits Endophilin B2 to the Cytoskeleton for Activity-Dependent Endocytosis of Synaptic Glutamate Receptors

Highlights

- CPG2 couples the endocytic machinery to the F-actin cytoskeleton through EndoB2
- CPG2 and EndoB2 interact to facilitate activity-dependent internalization of GluRs

Authors

Sven Loebrich, Marc Robert Benoit, Jaclyn Aleksandra Konopka, Jeffrey Richard Cottrell, Joanne Gibson, Elly Nedivi

Correspondence

nedivi@mit.edu

In Brief

Loebrich et al. show that CPG2 acts as a structural and functional link between the F-actin cytoskeleton and the endocytic machinery at excitatory postsynaptic sites. They identify a new component of the endocytic complex, EndoB2, as a CPG2 partner required for activity-dependent glutamate receptor endocytosis, a key aspect of synaptic plasticity.

Loebrich et al., 2016, Current Biology *26*, 1–13
February 8, 2016 ©2016 Elsevier Ltd All rights reserved
http://dx.doi.org/10.1016/j.cub.2015.11.071

CellPress

Please cite this article in press as: Loebrich et al., CPG2 Recruits Endophilin B2 to the Cytoskeleton for Activity-Dependent Endocytosis of Synaptic Glutamate Receptors, Current Biology (2016), http://dx.doi.org/10.1016/j.cub.2015.11.071

Current Biology
Article

CellPress

CPG2 Recruits Endophilin B2 to the Cytoskeleton for Activity-Dependent Endocytosis of Synaptic Glutamate Receptors

Sven Loebrich,[1] Marc Robert Benoit,[1] Jaclyn Aleksandra Konopka,[1] Jeffrey Richard Cottrell,[1] Joanne Gibson,[1] and Elly Nedivi[1,*]
[1]Picower Institute for Learning and Memory, Massachusetts Institute of Technology, 43 Vassar Street, Cambridge, MA 02139, USA
*Correspondence: nedivi@mit.edu
http://dx.doi.org/10.1016/j.cub.2015.11.071

SUMMARY

Internalization of glutamate receptors at the postsynaptic membrane via clathrin-mediated endocytosis (CME) is a key mechanism for regulating synaptic strength. A role for the F-actin cytoskeleton in CME is well established, and recently, PKA-dependent association of candidate plasticity gene 2 (CPG2) with the spine-cytoskeleton has been shown to mediate synaptic glutamate receptor internalization. Yet, how the endocytic machinery is physically coupled to the actin cytoskeleton to facilitate glutamate receptor internalization has not been demonstrated. Moreover, there has been no distinction of endocytic-machinery components that are specific to activity-dependent versus constitutive glutamate receptor internalization. Here, we show that CPG2, through a direct physical interaction, recruits endophilin B2 (EndoB2) to F-actin, thus anchoring the endocytic machinery to the spine cytoskeleton and facilitating glutamate receptor internalization. Regulation of CPG2 binding to the actin cytoskeleton by protein kinase A directly impacts recruitment of EndoB2 and clathrin. Specific disruption of EndoB2 or the CPG2-EndoB2 interaction impairs activity-dependent, but not constitutive, internalization of both NMDA- and AMPA-type glutamate receptors. These results demonstrate that, through direct interactions with F-actin and EndoB2, CPG2 physically bridges the spine cytoskeleton and the endocytic machinery, and this tripartite association is critical specifically for activity-dependent CME of synaptic glutamate receptors.

INTRODUCTION

Clathrin-mediated endocytosis (CME) of postsynaptic glutamate receptors is central for implementing long-term depression (LTD) and other forms of synaptic plasticity [1]. CME requires functional and temporal orchestration of numerous participating endocytic proteins. There is significant evidence that, in mammalian cells, CME relies on an active F-actin cytoskeleton at various stages in the life cycle of an endocytic vesicle (reviewed in [2, 3]). Despite the demonstrated functional link between F-actin and CME, little is known about the mechanisms underlying the coupling of these modules. Endocytic proteins, such as Hip-1 and dynamin, are known to interact indirectly with the actin cytoskeleton [4, 5], whereas others can associate with actin nucleating factors (reviewed in [2, 6]). However, none of these interactions were shown to be required for CME of synaptic glutamate receptors. Candidate plasticity gene 2 (CPG2) is an activity-regulated gene product of *Syne1*, enriched at endocytic zones within dendritic spines [7]. PKA-dependent association of CPG2 with F-actin is required for glutamate receptor internalization [8]. Here, we identify a direct physical interaction between CPG2 and EndoB2 and show that, by recruitment of this previously uncharacterized component of the endocytic machinery, CPG2 tethers the endocytic apparatus to the F-actin cytoskeleton in dendritic spines. We further show that this interaction is essential specifically for activity-dependent, but not constitutive, internalization of synaptic glutamate receptors.

RESULTS

Identification of Endophilin B2 as a CPG2 Binding Partner

We previously showed that CPG2 is enriched at the endocytic zone in dendritic spines, where it regulates constitutive and activity-dependent internalization of synaptic glutamate receptors [7]. Two coiled-coil regions in the CPG2 C terminus form a bipartite F-actin-binding motif critical for its function in regulating endocytosis [8]. However, the mechanism by which the CPG2/F-actin association couples the endocytic process to the spine cytoskeleton remains unclear. In an unbiased approach to identifying CPG2-binding proteins that might be part of, or closely associated with, the endocytic machinery, we immuno-isolated CPG2 from rat brain, resolved the samples by SDS-PAGE, and stained with silver nitrate for proteins that co-precipitate with CPG2 (Figure 1A). CPG2 was detected as a band of the expected ~105-kD size. One additional band at ~56 kD co-precipitated with CPG2, but not with control IgG (Figure 1A, left panel, arrow). After excision and tryptic digest, mass spectrometry identified the ~56-kD band as the BAR-domain-containing protein, endophilin B2, hereby referred to as EndoB2.

We validated the interaction between CPG2 and EndoB2 by testing the ability of CPG2 to pull down EndoB2 in a heterologous

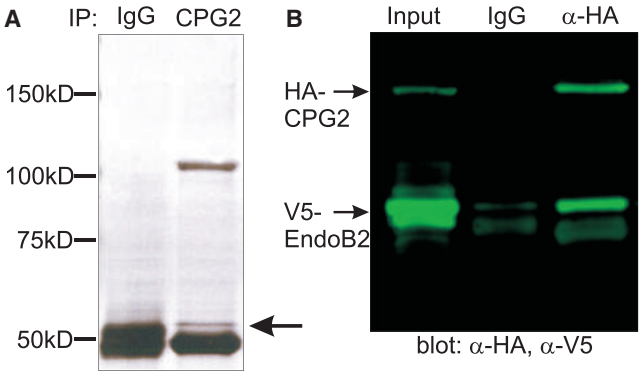

Figure 1. EndoB2 Is a CPG2 Binding Partner

(A) Silver stain of co-immunoprecipitations from rat brain using control mouse IgG (left lane) or anti-CPG2 monoclonal antibody (right lane). Note CPG2 at ~105 kD and the additional band at ~56 kD (arrow). This band was excised and identified as EndoB2 using mass spectrometry.

(B) Co-immunoprecipitation of V5-tagged EndoB2 with HA-tagged CPG2 from soluble fractions of co-transfected HEK293T cell lysates.

expression system. HEK293T cells were co-transfected with vectors encoding V5-tagged EndoB2 and HA-tagged full-length CPG2. Western blotting confirmed HA-CPG2 and V5-EndoB2 expression in HEK293T cell lysates (Figure 1B, input) and enrichment for HA-CPG2 by immunoprecipitation with α-HA antibodies. Consistent with EndoB2 binding to CPG2, V5-tagged EndoB2 specifically co-immunoprecipitated with HA-CPG2, but not with control IgG (Figure 1B). Together, these results identify EndoB2 as a CPG2 binding partner and demonstrate that this interaction can be recapitulated in a heterologous expression system.

CPG2 Interacts Directly with EndoB2 through a Coiled-Coil Motif

To identify the minimal binding region in CPG2 required to mediate its association with EndoB2, we performed a structure-function analysis, co-expressing V5-tagged EndoB2 in HEK293T cells with numerous HA-tagged CPG2 truncations (Figure 2A). The CPG2 spectrin repeat and the first coiled-coil were dispensable for association with EndoB2 because the N-terminal half of the protein (fragment N1) failed to bind V5-EndoB2 (Figure 2B, top). In contrast, the C-terminal C6 fragment was highly effective in co-precipitating EndoB2. Further dissection of the C terminus showed that a C5 fragment harboring the second and third CPG2 coiled-coil motifs is sufficient for association with EndoB2 (Figure 2B, middle). A construct (M1) containing only the middle CPG2 coiled-coil domain could also precipitate V5-EndoB2, suggesting that amino acids 798–876 in CPG2 represent the minimal binding region for association with EndoB2. This minimal binding region was defined as CPG2 fragment M2. Due to its small size, the HA-tagged M2 fragment was difficult to immunoprecipitate directly. We therefore inserted a GFP molecule between the HA tag and the M2 fragment, to increase its size, allowing its immunoprecipitation with the anti-HA antibody (Figure 2B, bottom, input). In this context, the M2 fragment was able to co-immunoprecipitate V5-tagged EndoB2, suggesting CPG2 amino acids 798–876 are sufficient to bind EndoB2 (Figure 2B, bottom).

To identify the region in EndoB2 mediating its association with CPG2, we performed a similar structure-function analysis, co-expressing HA-tagged full-length CPG2 with FLAG-tagged EndoB2 truncations in HEK293T cells. Endophilins comprise an N-terminal BAR domain required for association with the plasma membrane, a variable linker region, and a C-terminal SH3 protein-protein interaction domain for association with proline-rich regions [9]. The BAR domain is composed of three helical stretches (H1–3) of variable length (Figure 2C). We tested numerous truncations of EndoB2 and found that the SH3 domain is insufficient for association with CPG2 (not shown). A construct harboring most of, but not the entire, BAR domain of EndoB2 (N152) also failed to associate with CPG2 (Figure 2D). In contrast, binding to CPG2 was reconstituted in a construct expressing 34 additional amino acids (N186), restoring the full second helical region in the BAR domain of EndoB2. These data suggest that CPG2 and EndoB2 bind each other directly via a 78-amino-acid region in CPG2 encompassing the second coiled-coil and a 34-amino-acid region within the second helical segment of the EndoB2 BAR domain.

CPG2 and EndoB2 Interact with Each Other at Synapses

We next tested for an endogenous CPG2-EndoB2 interaction in neurons. Cultured hippocampal neurons were co-stained using antibodies against both CPG2 and EndoB2. Consistent with the role of both proteins in synaptic CME, endogenous EndoB2 and CPG2 co-localized in dendritic spines (Figure 3A). We quantified this co-localization and found that more than two-thirds of CPG2 puncta were positive for EndoB2 (Figure 3B). To test whether the two proteins interact at this locale, we prepared synaptoneurosomes (shown as enriched for PSD95; Figure 3E) from rat brain and performed immunoprecipitations (5% of input fraction shown in Figure 3D). An antibody against EndoB2, but not control IgG, showed co-purification of CPG2 (Figure 3C, left). This antibody is specific to EndoB2: it recognizes a ~56-kD band from rat whole brain lysate that is not present when the antibody is pre-exposed to the immunogenic peptide (Figure 3F). Furthermore, the antibody recognizes V5-tagged EndoB2, but not endophilin A3 purified from HEK239T cell lysates (Figure 3G). Co-immunoprecipitation in the reverse direction with a CPG2-specific monoclonal antibody [7] specifically co-immunoprecipitated EndoB2 (Figure 3C, right). Thus, CPG2 is physically associated with EndoB2 in dendritic spines.

CPG2 Acts as a Physical Linker between EndoB2 and the F-Actin Cytoskeleton

We previously showed that CPG2 associates with F-actin in dendritic spines [8]. One possibility is that CPG2 independently interacts either with F-actin or EndoB2 and that both interactions are required for synaptic glutamate receptor CME. A more interesting alternative is that CPG2 mediates a tripartite interaction, simultaneously binding EndoB2 and F-actin. By acting as a physical linker between the two, CPG2 would effectively tether EndoB2 and the endocytic machinery to the F-actin cytoskeleton. To investigate this possibility, we performed an in vitro F-actin-binding assay. In brief, globular actin was allowed to polymerize in the presence of ATP under high salt conditions. Plasmids containing the EndoB2 or CPG2 ORF were transcribed and translated in vitro using a reticulocyte lysate in the presence

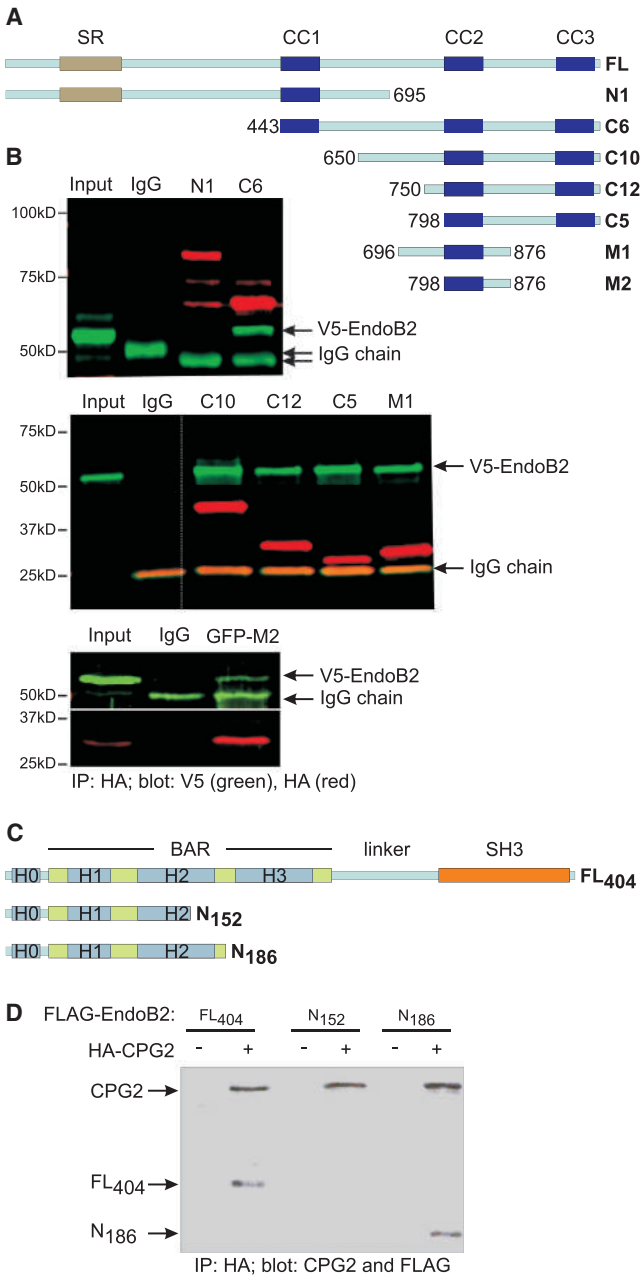

Figure 2. Mapping of CPG2 and EndoB2 Interaction Domains

(A) Schematic of the CPG2 protein and its predicted motifs (top). Amino acid position start and end sites for N-, C-terminal, and middle (M) truncations are indicated. A spectrin repeat (SR) and three coiled-coils (CC1–3) are annotated. FL, full length.

(B) Structure-function analysis using immunoprecipitation of V5-tagged EndoB2 co-expressed with different HA-tagged CPG2 truncations. (Top) The capacity to co-immunoprecipitate V5-tagged EndoB2 resides in the C-terminal half of CPG2. (Middle) Fine mapping suggests that EndoB2 binds to amino acids 798–876 in CPG2. Note: the light chains of the antibodies used for immunoprecipitation are recognized by the α-mouse secondary antibody and appear yellow. Dotted line indicates that lanes between IgG and C10 rows were excised for presentation. (Bottom) Confirmation that CPG2 amino acids 798–876 (M2) are sufficient to co-immunoprecipitate EndoB2 is shown. The fragment was expressed as a fusion to GFP to help with immunoprecipitation.

(C) Schematic of EndoB2 protein domain structure (top) and FLAG-tagged EndoB2 truncation constructs used to map its interaction domain with CPG2. Helical segments (H0–H3, gray), the BAR-domain (green), the linker region, and the SH3 domain (orange) are depicted.

(D) Structure-function analysis using immunoprecipitation of HA-tagged CPG2 co-expressed in combination with different FLAG-tagged EndoB2 truncations reveals that CPG2 binds to amino acids 152–186 in EndoB2.

of ^{35}S-radiolabeled methionine and added to the polymerized actin. Actin filaments were then collected by ultracentrifugation, and association of EndoB2 with F-actin was assessed by quantifying the ratio of autoradiography signal in the pellet versus supernatant. In the absence of CPG2, EndoB2 did not precipitate with actin filaments (Figure 4A, left panel). Consistent with our earlier findings, CPG2 showed robust association with F-actin [8]. When CPG2 was co-expressed with EndoB2, a significantly greater fraction of EndoB2 associated with F-actin (Figures 4A, right panel, and 4B). These results show that, in vitro, EndoB2 does not bind F-actin but can be recruited to F-actin by CPG2.

To test whether endogenous EndoB2 was recruited to the cytoskeleton by endogenous CPG2 in dendritic spines, lentiviral-infected hippocampal neurons expressing control or a CPG2 knockdown construct were treated with ice-cold Triton X-100. This solubilizes plasma and internal membranes and washes away cytosolic components, leaving the cytoskeleton and its associated proteins intact [8, 10]. After extraction with Triton X-100, neurons were fixed and labeled with rhodamine phalloidin to visualize the actin cytoskeleton and immunostained to visualize endogenous EndoB2 (Figure 4C). Knockdown of endogenous CPG2 led to a significant decrease in EndoB2 immunoreactivity in F-actin-labeled spines after extraction (Figure 4D).

We previously showed that CPG2 associates with F-actin in a PKA-dependent manner. Preventing PKA phosphorylation of CPG2, either by pharmacological blockade of PKA or through mutation of the target serines on CPG2, abrogates glutamate receptor internalization, suggesting CPG2's association with F-actin is critical for its function [8]. A CPG2 S890A/S913A double mutant (PKAabol) that cannot be phosphorylated by PKA at these specific sites fails to bind F-actin, whereas a CPG2 phosphomimetic S890E/S913E double mutant (PKAmim) constitutively associates with the spine cytoskeleton [8]. To test whether CPG2's PKA target sites are critical for anchoring EndoB2 to the F-actin cytoskeleton, cultured hippocampal neurons were infected with a lentivirus that knocks down endogenous CPG2 and replaces it with either wild-type CPG2, PKAabol, or PKAmim. After Triton X-100 extraction, knockdown of endogenous CPG2 and replacement with the PKAabol mutant could not rescue loss of EndoB2 binding to the cytoskeleton (Figures 4E and 4F). In contrast, replacing CPG2 with the constitutively active F-actin-binding PKAmim mutant increased the amount of EndoB2 bound to F-actin (Figures 4E and 4F). The increase above WT was not statistically significant, consistent with our earlier observation that CPG2 seems to be predominantly actin bound [8].

CPG2 Tethers Endocytic Machinery to the Cytoskeleton through EndoB2

To examine whether this physical link that CPG2 forms between the cytoskeleton and EndoB2 extends to other components of

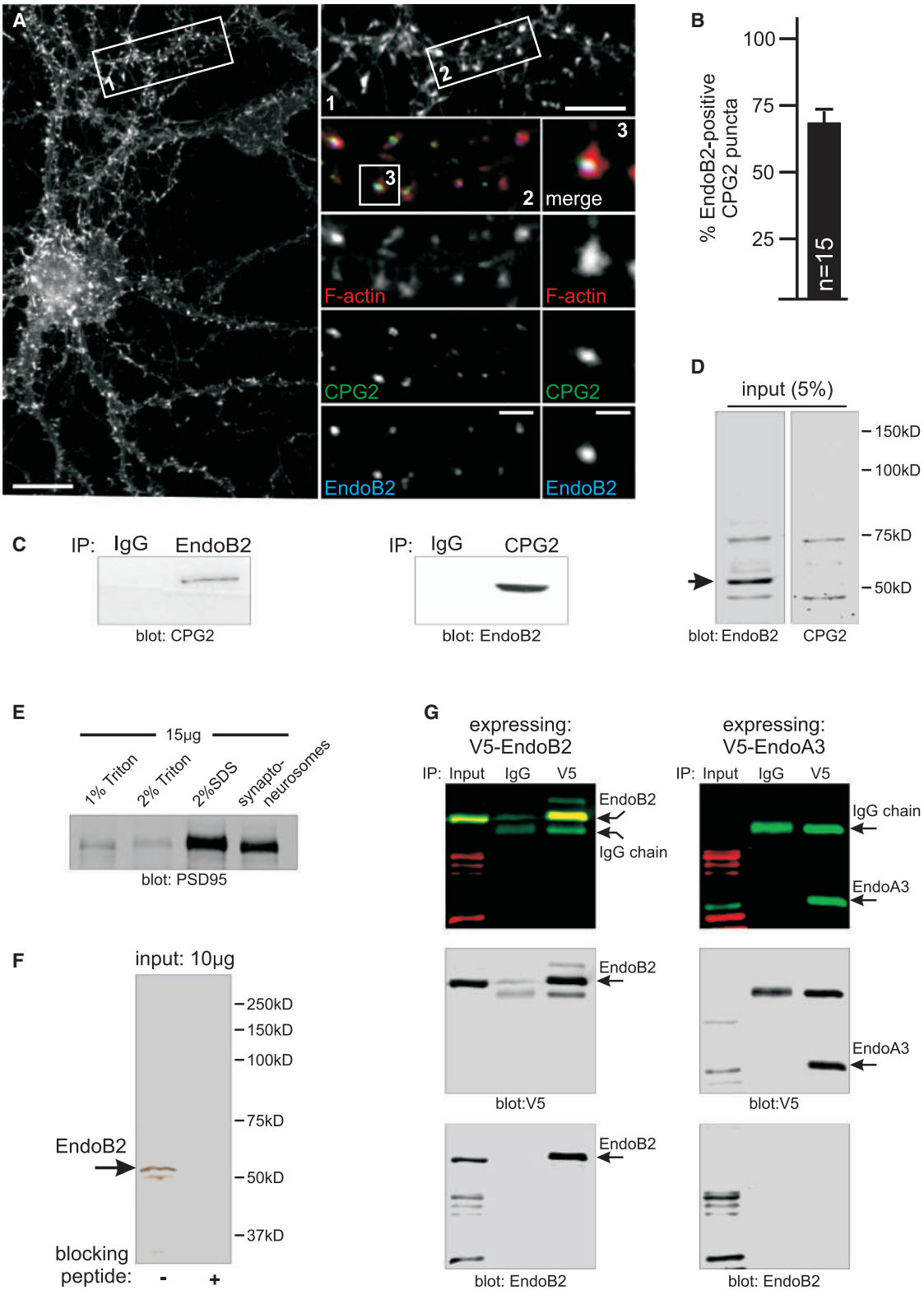

Figure 3. Endogenous CPG2 and Endogenous EndoB2 Co-localize and Bind Each Other at Synapses

(A) Immunocytochemistry of cultured hippocampal neurons shows co-localization of CPG2 and EndoB2 in dendritic spines. (Left) A representative cell is shown, stained with rhodamine phalloidin to visualize F-actin (red). The scale bar represents 30 µm. (Right) Box 1 from left, shown in consecutive magnifications to visualize F-actin only (top; scale bar: 10 µm), as well as CPG2 (green) and EndoB2 (blue), boxes 2 (scale bar: 5 µm) and 3 (scale bar: 2 µm) are shown. High magnification of a single dendritic spine reveals overlapping localization of CPG2 and EndoB2 immunoreactivity.

(legend continued on next page)

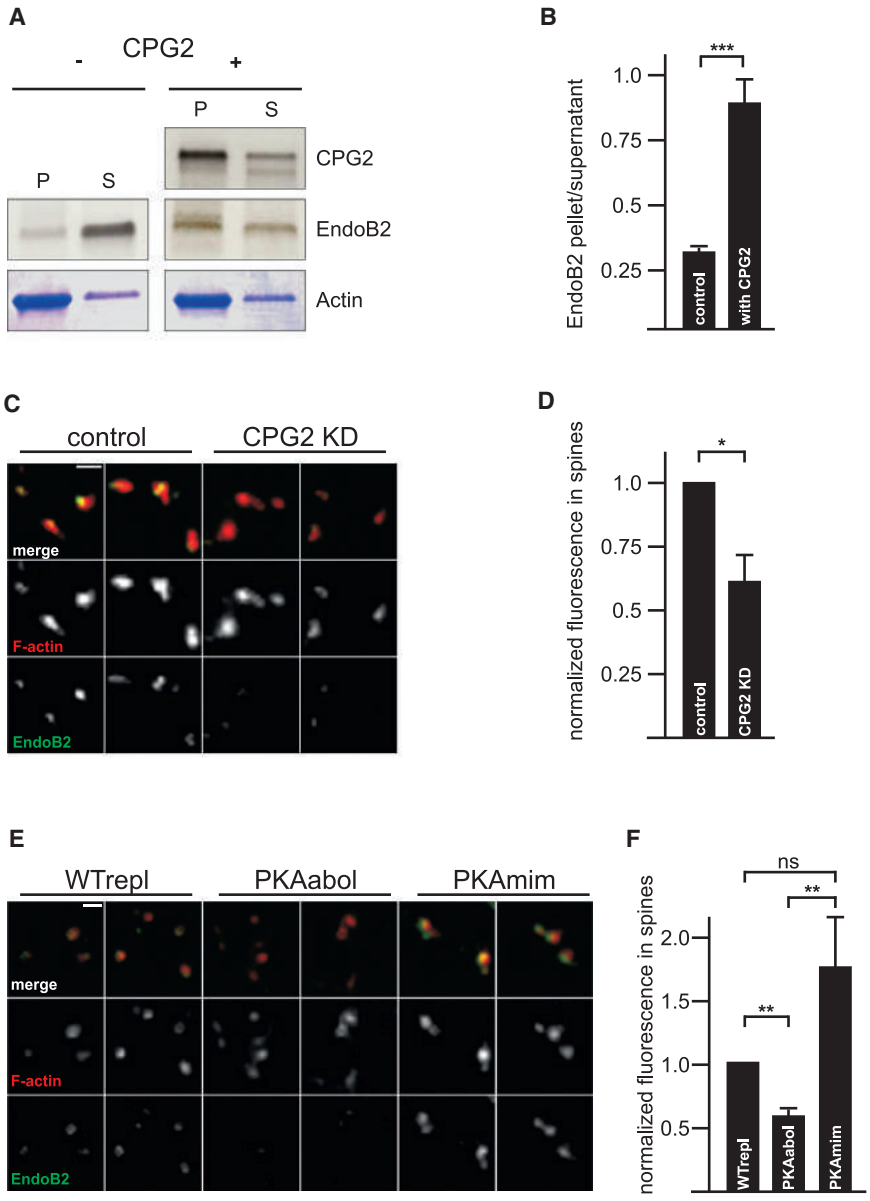

Figure 4. CPG2 Mediates EndoB2 Binding to the F-Actin Cytoskeleton in a PKA-Dependent Manner

(A) Autoradiography of ^{35}S-labeled CPG2 or EndoB2 in pellet (P) or supernatant (S) fractions after ultracentrifugation of in vitro polymerized F-actin. Coomassie stain of actin is shown at bottom. EndoB2 does not bind to F-actin in the absence of CPG2 (left panels) but is recruited to the F-actin pellet when CPG2 is present (right panels).

(B) Quantification of EndoB2 intensity ratio in pellet versus supernatant ± SEM: 0.30 ± 0.018; n = 7 without CPG2 versus 0.89 ± 0.094; n = 8 with CPG2; ***p < 0.001; Student's t test.

(C) Representative immunofluorescence images of dendritic spines from cultured hippocampal neurons infected with either control or CPG2 knockdown virus. Spine heads are visualized by staining for F-actin; endogenous EndoB2 is immuno-stained in green. The scale bar represents 2 μm.

(D) Quantification of EndoB2 fluorescence intensity in dendritic spines shown as mean intensity ± SEM normalized to control: 0.61 ± 0.11; n = 3 experiments: 19 control cells, 24 CPG2 knockdown cells; *p < 0.05; Student's t test.

(E) Representative immunofluorescence images of dendritic spines from cultured hippocampal neurons infected with a virus harboring a CPG2 knockdown hairpin and either a control or mutated CPG2 replacement construct. PKAabol, a phospho-incompetent S890A/S913A mutant, unable to be phosphorylated by PKA, fails to bind F-actin. PKAmim, an S890E/S913E mutant that mimics constitutive PKA phosphorylation. Spine heads are visualized by staining for F-actin; endogenous EndoB2 is immuno-stained in green. The scale bar represents 2 μm.

(F) Quantification of EndoB2 fluorescence intensity in dendritic spines shown as normalized mean intensity ± SEM: relative to wild-type replacement CPG2: 0.59 ± 0.05 for PKAabol, n = 3 experiments: 19 cells for wild-type, 24 cells for PKAabol; 1.81 ± 0.38 for PKAmim, n = 3 experiments: 16 cells. **p < 0.01; Student's t test; ns, not significant.

the endocytic machinery, we first confirmed that EndoB2 and clathrin heavy chain co-localize in dendritic spines. Triple labeling of V5-EndoB2, clathrin-GFP, and PSD95-tdTomato expressed in cultured neurons, revealed that EndoB2 and clathrin co-localize in the direct vicinity of the postsynaptic density (Figure 5A). Further, CPG2 was found to co-localize with endogenous clathrin in dendritic spines (Figure 5B). These results show that CPG2, clathrin heavy chain, and EndoB2 co-localize at the endocytic zone in postsynaptic compartments.

We next asked whether cytoskeletal anchoring by CPG2 extends beyond EndoB2 to other components of the endocytic machinery. We tested whether clathrin heavy chain, a core

(B) Quantification of percent CPG2 puncta staining positive for endophilin B2 represented as mean ± SEM.

(C) Immunoprecipitation of EndoB2 from rat brain synaptoneurosomes co-precipitates CPG2 (left). Reverse co-immunoprecipitations of EndoB2 with CPG2 from synaptoneurosomes are shown on the right.

(D) Input material for co-immunoprecipitation experiments. Five percent of offered material was loaded to estimate percentage of co-immunoprecipitation. Note that no band is detected for CPG2 in input lane.

(E) Western blot probed for the postsynaptic density marker PSD95 to assess enrichment of synaptic components in synaptoneurosome preparation, compared to several stages of purification in a classical PSD preparation.

(F) Test for antibody specificity of rabbit anti-EndoB2 antibody. The antibody recognizes a prominent band at ~56 kD in 10 μg of rat whole-brain lysate (left lane). This band can be suppressed by preincubation with a specific blocking peptide (right lane).

(G) The anti-EndoB2 antibody readily recognizes V5-tagged EndoB2 heterologously expressed in HEK293T cells (left panel). The antibody fails to recognize V5-tagged endophilin A3, even after enrichment by immunoprecipitation with anti-V5 antibodies (right panel).

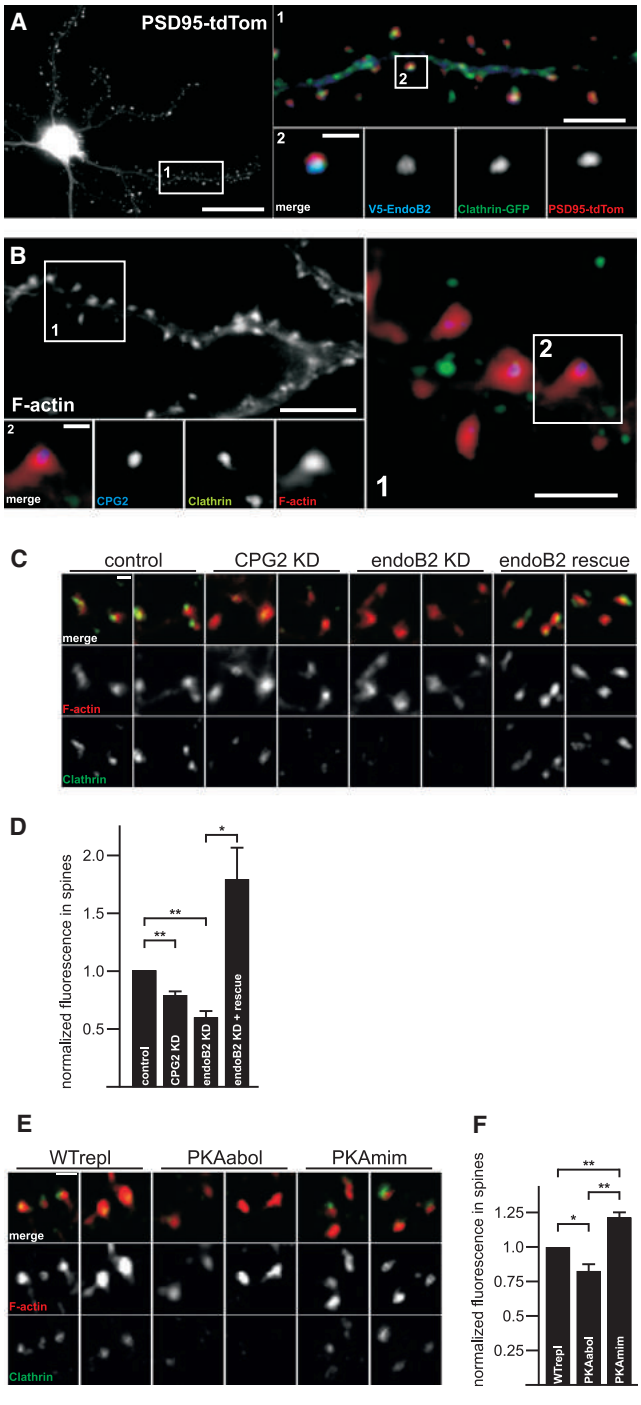

Figure 5. CPG2 and EndoB2 Co-localize and Recruit Components of the Endocytic Machinery to F-Actin

(A) Immuno-cytochemistry on cultured hippocampal neurons transfected with plasmids encoding V5-EndoB2, GFP-clathrin, and tdTomato-PSD95. (Left panel) Black and white image of tdTomato-PSD95 signal to visualize overall neuronal morphology is shown (scale bar: 30 μm). (Right) Box 1 from left is shown in color: tdTomato-PSD95 (red); clathrin-GFP (green); and V5-EndoB2 (blue; scale bar: 10 μm). (Box 2) Further magnification reveals that V5-EndoB2 and clathrin-GFP co-localize with each other lateral to the postsynaptic density (scale bar: 2 μm).

(B) Immunocytochemistry on cultured hippocampal neurons. (Top left image) Black and white image of rhodamine phalloidin stain to visualize F-actin in a dendritic segment is shown (scale bar: 15 μm). A smaller segment is boxed and shown in color in the right image (scale bar: 5 μm). (Lower panel) Boxed region in right image, shown in the lower left panel, is separated into individual channels in lower right panels. F-actin is depicted in red, clathrin heavy chain staining in green, and CPG2 staining in blue (scale bar: 2 μm).

(C) Representative immunofluorescence images of dendritic spines from cultured hippocampal neurons infected with either control, CPG2 knockdown virus, EndoB2 knockdown virus (see Figure S1 for characterization of EndoB2 knockdown hairpins), or a rescue virus for EndoB2 knockdown also expressing knockdown-resistant EndoB2. Cells were treated with detergent to release cellular components not associated with the cytoskeleton and then fixed and stained with rhodamine phalloidin to visualize F-actin (red) or anti-clathrin heavy chain (green; scale bar: 2 μm).

(D) Quantification of fluorescence intensity in F-actin-positive spine heads normalized to control following extraction, shown as mean intensity ± SEM: control versus CPG2 KD: 0.79 ± 0.04, n = 3 experiments, 12 control cells, 15 CPG2 knockdown cells; control versus EndoB2 KD: 0.59 ± 0.06, n = 3 experiments, 12 control cells, 15 EndoB2 knockdown cells; EndoB2 KD versus rescue: 1.78 ± 0.28, n = 4 experiments, 20 rescue cells. *p < 0.05; **p < 0.01; Student's t test.

(E) Representative immunofluorescence images of dendritic spines from cultured hippocampal neurons infected with either control or CPG2 replacement virus that knocks down endogenous CPG2 and replaces it with wild-type CPG2 (WTrepl), a phospho-incompetent S890A/S913A CPG2 mutant (PKAabol) that cannot be phosphorylated by PKA and fails to bind to F-actin, or a S890E/S913E phosphomimetic CPG2 mutant (PKAmim) that acts as if constitutively phosphorylated by PKA, constitutively binding actin. Spine heads are visualized by staining for F-actin; endogenous clathrin heavy chain is immuno-stained in green (scale bar: 2 μm).

(F) Quantification of clathrin heavy chain fluorescence intensity in dendritic spines, normalized to control and shown as mean intensity ± SEM: PKAabol: 0.83 ± 0.06, n = 3 experiments, 15 cells for WTrepl, 19 cells for PKAabol; PKAmim: 1.22 ± 0.04, n = 3 experiments, 15 cells for PKAmim. *p < 0.05; **p < 0.01; Student's t test.

component of the endocytic machinery, was cytoskeletally attached and whether this attachment was CPG2 dependent. Triton X-100 extracted neurons were infected with lentivirus expressing a control construct or the CPG2 knockdown construct [7, 8]. The intensity of clathrin heavy chain immunofluorescence in dendritic spines was significantly reduced when CPG2 was knocked down as compared to control (Figures 5C, left, and 5D).

To test whether clathrin anchoring to the cytoskeleton via CPG2 is mediated through EndoB2, we designed three independent short interfering hairpins against EndoB2 (Figure S1A). Two of these, hairpins 62 and 379, showed robust knockdown of EndoB2 protein in cultured neurons (Figures S1B–S1G). Other synaptic proteins were unaffected (Figure S1H), and EndoB2 expression was fully rescued by a replacement construct co-expressing EndoB2 with a silent mutation conferring hairpin resistance, together with the hp62 hairpin (Figure S1I), confirming that knockdown was specific. Similar to the effect of knocking down CPG2, knockdown of EndoB2 using hp62 significantly reduced clathrin heavy chain association with the spine cytoskeleton after Triton X-100 extraction (Figures 5C, right, and 5D). Clathrin cytoskeletal association could be rescued by the EndoB2 replacement construct (Figures 5C and 5D).

Because CPG2's association with F-actin, and recruitment of EndoB2 to the cytoskeleton, are dependent on phosphorylation of CPG2 by PKA on specific serine residues, we predicted that clathrin heavy chain cytoskeletal attachment would be similarly dependent on CPG2 phosphorylation at these sites. Indeed, endogenous CPG2 knockdown and replacement with either

the PKAabol or PKAmim mutants reduced or increased, respectively, clathrin heavy chain immunoreactivity in association with the spine cytoskeleton in Triton X-100 extracted neurons (Figures 5E and 5F).

Together, these data demonstrate that CPG2 physically anchors components of the endocytic machinery to the F-actin cytoskeleton via direct interaction with EndoB2 and that association of these components with the cytoskeleton is regulated by PKA-targeted phosphorylation of CPG2.

EndoB2 Is Required for Activity-Dependent Glutamate Receptor Internalization

CPG2 was previously shown to be required for both constitutive and activity-dependent glutamate receptor internalization [6]. Our finding that EndoB2 bridges between CPG2 and components of the endocytic machinery suggests it also plays a role in CME of synaptic glutamate receptors. To investigate this possibility, we performed a biochemical internalization assay to quantitatively assess glutamate receptor endocytosis in cultured cortical neurons that were uninfected or infected with lentivirus expressing tdTomato alone or expressing tdTomato along with EndoB2 hp62. Constitutive internalization of AMPA- and NMDA-type glutamate receptors seemed unaffected by EndoB2 KD (Figures 6A and 6B).

We next tested EndoB2's role in activity-dependent glutamate receptor internalization by performing the receptor internalization assay after increasing global activity in cortical cultures by treatment with picrotoxin, a $GABA_A$ receptor open channel blocker. Picrotoxin treatment has been shown to induce robust internalization of glutamate receptors, in particular GluA1-containing AMPA receptors [11]. We found a similar result, an almost 3-fold increase in GluA1 internalization in response to picrotoxin (Figure S2). Surprisingly, EndoB2 knockdown resulted in a significant decrease in activity-dependent internalization not only of GluA1 glutamate receptor subunits but also of GluA2 and GluN1 subunits (Figures 6C and 6D).

The biotinylation assay represents internalization of all surface receptors, both synaptic and non-synaptic. To examine whether the role of EndoB2 in activity-dependent glutamate receptor trafficking was relevant to synaptic receptors, we used a fluorescence-based assay for surface labeling of live-cultured hippocampal neurons with antibodies directed against the extracellular N terminus of GluA1. GluA1 surface labeling of neurons infected with a tdTomato-expressing control construct shows clear staining of synaptic puncta. Application of the glutamate analog NMDA, a paradigm of chemical LTD, results in activity-mediated GluA1 receptor internalization visualized by a significant decrease in puncta intensity (Figures 6E and 6F). Knockdown of either CPG2 or EndoB2 prevented NMDA-induced GluA1 internalization (Figures 6E and 6F). The effect of CPG2 knockdown on NMDA-induced GluA1 internalization could be rescued by expression of a hairpin-resistant CPG2 or by expression of the PKAmim mutant, but not by expression of the PKAabol that prevents CPG2 cytoskeletal association (Figure S3).

Whereas these results do not rule out a role for the CPG2-EndoB2 interaction in internalization of non-synaptic receptors, they do demonstrate that the CPG2-EndoB2 interaction is important for facilitating activity-dependent internalization of synaptic glutamate receptors, consistent with enrichment of both CPG2 and EndoB2 to dendritic spines.

Association of CPG2 with EndoB2 Is Required for Activity-Dependent Glutamate Receptor Internalization

To determine whether the role of EndoB2 in activity-dependent endocytosis of glutamate receptors is dependent on its interaction with CPG2, we disrupted the binding of endogenous EndoB2 and CPG2 by overexpressing M2, the minimal CPG2 fragment required for EndoB2 binding (Figures 2A and 2B). M2 (amino acids 798–876) fused to GFP, or GFP alone, was cloned into a lentiviral vector (Figure 7A). Expression of GFP-M2, but not GFP alone, completely prevented co-immunoprecipitation of V5-EndoB2 with HA-CPG2 in HEK293T cell lysates (Figure 7B), demonstrating that it can abrogate CPG2 binding to EndoB2. We then performed the biochemical internalization assay on cultured cortical neurons that were either uninfected or infected with lentivirus expressing GFP alone or GFP fused to the M2 fragment. Similar to EndoB2 KD, overexpression of the GFP-M2 fragment showed no effect on constitutive cycling of AMPA- or NMDA-type glutamate receptors (Figures 7C and 7D).

In contrast, the presence of GFP-M2 significantly impaired activity-dependent internalization of GluA2, GluN1, and GluA1 in response to picrotoxin (Figures 7E and 7F). To confirm that disrupting the CPG2-EndoB2 interaction is relevant to synaptic glutamate receptor internalization, we again used the GluA1 surface-labeling assay. Surface staining of live-cultured hippocampal neurons infected with only GFP showed a robust decrease in punctate GluA1 immunoreactivity in response to NMDA treatment (Figures 7G and 7H), whereas neurons infected with GFP-M2 showed no NMDA-dependent GluA1 receptor internalization (Figures 7G and 7H). These data demonstrate that the association between CPG2 and EndoB2 is critical for activity-dependent, but not constitutive, glutamate receptor internalization.

DISCUSSION

The EndoB2-CPG2 Interaction as a Structural Bridge between F-Actin and the Endocytic Machinery

Here, we describe a direct interaction between CPG2 and EndoB2 that structurally tethers EndoB2 and, through it, other components of the endocytic machinery such as clathrin, to the F-actin cytoskeleton in dendritic spines. We show that this interaction is critical for activity-dependent internalization of synaptic glutamate receptors. Many studies have implicated the actin cytoskeleton in mammalian CME, predominantly through pharmacological blockade of F-actin polymerization or filament turnover [12–14] (reviewed in [3]). In particular, CME of synaptic glutamate receptors is known to require actin remodeling [15–17]. Some actin-associated proteins have been shown to regulate AMPA or NMDA receptor trafficking either directly or indirectly, e.g., α-actinin via the LIM- and PDZ-domain containing protein RIL [18] or the Arp2/3 complex by association with Shank3 [19]. Yet how the functional requirement for actin relates to the endocytic machinery at the molecular level has been unclear.

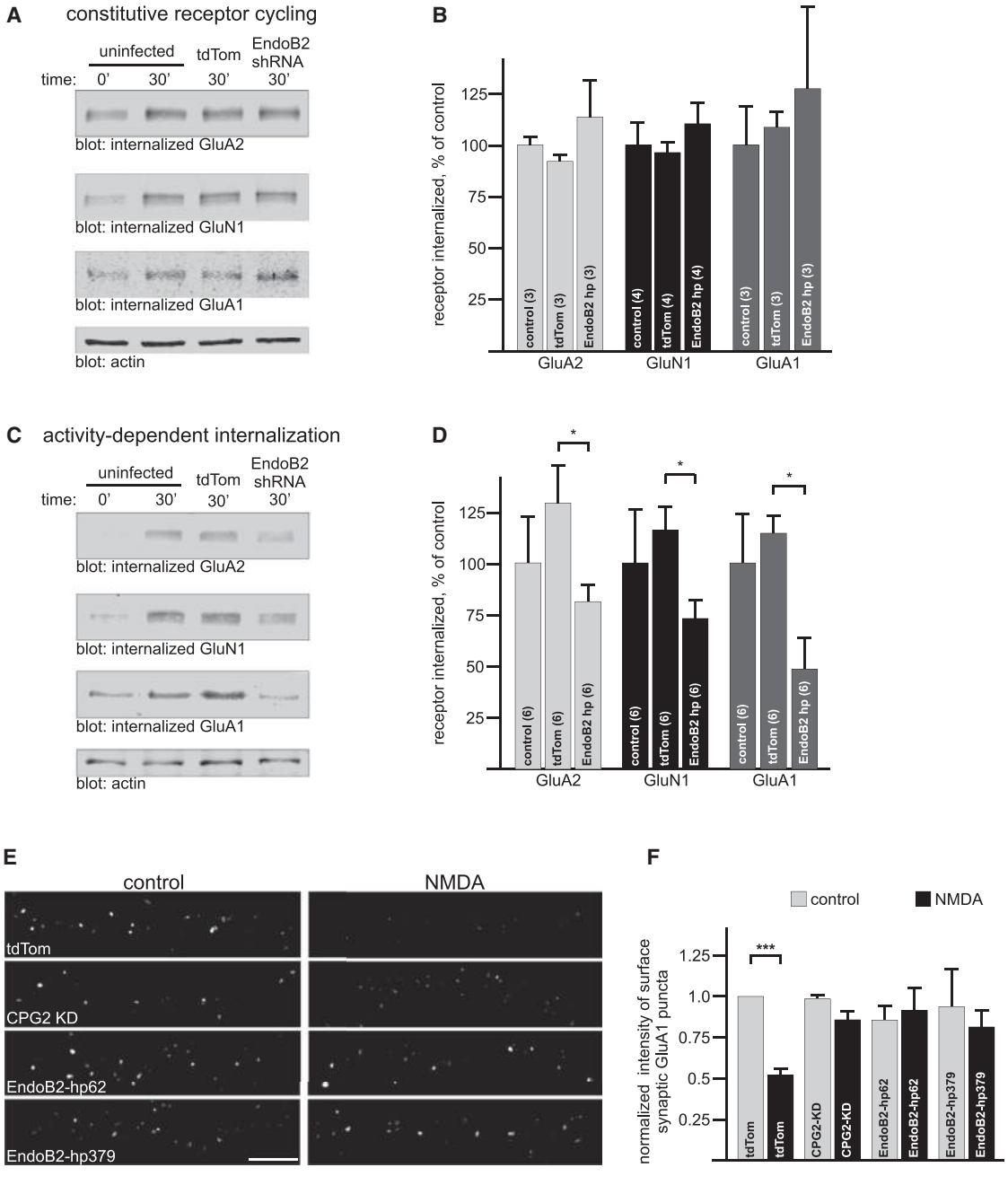

Figure 6. EndoB2 Is Required for Activity-Dependent, but Not Constitutive, Internalization of AMPA- and NMDA-Type Glutamate Receptors

(A) Constitutive cycling of glutamate receptor subunits measured in a biotinylation assay: surface proteins of cultured cortical neurons infected with indicated virus were labeled at 4°C with a cleavable biotin tag. After 30 min at 37°C to allow for glutamate receptor internalization, remaining surface labels were stripped and internalized membrane proteins were affinity purified and probed on western blots for GluA2, GluN1, and GluA1. Representative examples are shown as labeled. Bottom panel shows actin levels confirming equal input material.

(B) Quantification of constitutive receptor cycling in the biotinylation assay shown as percent of control ± SEM: 114% ± 18% for GluA2, p = 0.34, Student's t test; 110% ± 10% for GluN1, p = 0.27, Student's t test; 127% ± 40% for GluA1, p = 0.67, Student's t test; n values indicated in parentheses for each condition.

(C) Activity-dependent internalization of glutamate receptors in the same biotinylation assay as described above but after treatment with 100 μM picrotoxin (see Figure S2 for effect of picrotoxin on internalization of AMPA receptor subunits).

(D) Quantification of activity-dependent internalization shown as percent of control ± SEM: 81% ± 8% for GluA2; 73% ± 9% for GluN1; 48% ± 16% for GluA1; n values indicated in parentheses for each condition. *p < 0.05; Student's t test.

(E) Immuno-staining of surface GluA1 in neurons infected with tdTomato alone, CPG2 hairpin, or endophilin B2 hairpins 62 and 379 under control conditions (left panel) or after NMDA-induced AMPA receptor internalization (right panel; see Figure S3 for effect of CPG2 PKA mutations on NMDA-induced synaptic AMPA receptor internalization). The scale bar represents 15 μm.

(legend continued on next page)

Several components of the endocytic machinery have been shown to interact indirectly with actin. For example, EndoB2 was shown to associate with the cytoskeletal linker protein plectin 1 [20] in non-neuronal cells. Dynamins can bind the F-actin-binding proteins profilin II [21], cortactin [22], Abp1 [23], SNX9 [24], and intersectin [25]. HIP1, which binds to clathrin and the adaptor complex [26] and plays a role in GluA1 internalization [27], can dimerize with its close relative HIP1R [5], an actin-binding protein required for CME [4]. The relevance of these interactions to glutamate receptor CME has not been demonstrated. We previously showed that CPG2 binds to F-actin at neuronal synapses [8]. Here, we show that CPG2 is also a direct binding partner of EndoB2, a member of the endophilin family whose role in CME has previously not been well characterized. We confirmed that EndoB2 is critical for CME of glutamate receptors and for recruitment of clathrin to the dendritic spine cytoskeleton. Through its interaction with EndoB2, CPG2 provides a direct structural link between the CME machinery and F-actin. By acting as a physical bridge between these two functional modules, CPG2 plays a key mechanistic role in internalization of synaptic glutamate receptors. Interestingly, Arc/Arg3.1 binds dynamin II and endophilin A3, and these interactions are critical for implementing LTD [28]. Arc/Arg3.1 can also associate with F-actin, in vitro [29]. However, its potential engagement with the cytoskeleton has been predominantly attributed to a role in the adjustment of spine size that accompanies long-term potentiation and memory consolidation [30, 31] (reviewed in [3]).

Endophilins as Part of the Endocytic Apparatus

Our data show that CPG2 binds directly to EndoB2. Endophilins have been thought to be important for early stages in the endocytic cycle, through recruiting other endocytic proteins via their SH3 domain or by inducing membrane curvature via their N-terminal BAR domain [32–34]. Recently, endophilins have been implicated in later stages of the endocytic cycle in different model systems, through their interaction with both dynamin [35] and the un-coating factor synaptojanin [36, 37]. Specifically, endophilin A2 has been implicated in clathrin-independent endocytosis [38, 39]: a specialized, dynamin-dependent fast internalization mechanism for specific extracellular cargo. These studies found little or no role for A3, B1, and B2 subtypes in clathrin-independent endocytosis. Although it is consistent with our data that the B2 subtype is involved with CME, these studies reveal an interesting phenomenon: that endophilin can distinguish between different modes of endocytosis. This could occur through interacting with different intracellular partners, depending on context. This is particularly interesting given our finding that EndoB2's role in CME is specific to activity-dependent, but not constitutive, GluR endocytosis. Because CPG2 seems to be more generally required for synaptic CME, it would likely engage a different partner for regulating constitutive glutamate receptor cycling.

Our observation that CPG2 not only recruits EndoB2 to F-actin but also anchors clathrin heavy chain at the spine cytoskeleton is consistent with a model whereby EndoB2 interfaces between CPG2 and other components of the CME machinery for activity-dependent GluR endocytosis. Loss of clathrin anchoring by CPG2 knockdown is likely secondary to loss of cytoskeletal association of EndoB2. Interestingly, deletion of synaptojanin, a well-known endocytic protein, leads to build-up of clathrin-coated vesicles [40], similar to the phenotype of CPG2 knockdown [7]. It is unknown whether CPG2 interacts with synaptojanin directly; however, both interact with endophilins. Similarly, Arc/Arg3.1 interacts with endophilin A3 and dynamins [28]. Because CPG2 and Arc/Arg3.1 share a number of similarities with respect to expression profile and regulation of glutamate receptor internalization, it is tempting to speculate that they might function through parallel mechanisms. Whether or not these mechanisms are partially redundant, e.g., whether Arc/Arg3.1 can also bind to EndoB2, remains to be addressed.

Regulation of Activity-Dependent versus Constitutive Receptor Internalization

Arc/Arg3.1 has also been shown to be critical for activity-dependent internalization of AMPA receptors [41–43], but not basal synaptic transmission [44]. Expression of a blocking peptide that prevents association of GluA2 with AP2, a core component of the endocytic machinery, disrupts Arc/Arg3.1-mediated receptor internalization [45] but has no effect on basal synaptic transmission [1]. Arc/Arg3.1 is also specific for evoked AMPAR, but not NMDAR, internalization [45]. In contrast, CPG2 is essential for both constitutive and activity-dependent internalization of both types of glutamate receptors [7], but blocking its interaction with EndoB2 is detrimental for activity-dependent CME of both AMPA and NMDA receptors.

Interfering with the CPG2-EndoB2 interaction using the M2 fragment of CPG2 attenuates glutamate receptor internalization when levels of excitation are enhanced by picrotoxin blockade of inhibition or when glutamatergic synapses are directly challenged with NMDA, a paradigm of chemical LTD. Although bath application of picrotoxin and NMDA is a crude approach compared to the single synaptic activation that likely happens in vivo in the context of activity-dependent synaptic plasticity, it allows visualization of a general response to increased activity that potentially reflects the capacity of individual synapses to respond in a given scenario [46, 47] (reviewed in [48]). The ability through EndoB2 to specifically disrupt activity-dependent glutamate receptor CME without effecting constitutive receptor cycling provides clues regarding the mechanistic relationship between these two processes that presumably engage much of the same cellular machinery.

During steady state, glutamate receptors cycle continuously between intracellular and surface compartments [49, 50]. In response to elevated neuronal activity, AMPARs get rapidly

(F) Quantification of synaptic GluA1 puncta intensity normalized to control ± SEM. NMDA treatment versus control: 0.55 ± 0.04, n = 3 experiments, 19 cells, 367 puncta for control; 19 cells, 417 puncta for NMDA induced, ***$p < 0.001$, Student's t test; NMDA treatment versus control for CPG2 KD: 0.86 ± 0.06, n = 3 experiments, 28 cells, 506 puncta for control; 30 cells, 463 puncta for NMDA induced. NMDA treatment versus control for hp62: 0.92 ± 0.14, n = 3 experiments, 28 cells, 500 puncta for control; 25 cells, 385 puncta for NMDA induced. NMDA treatment versus control for hp379: 0.81 ± 0.11, n = 3 experiments, 24 cells, 265 puncta for control; 27 cells, 495 puncta for NMDA induced.

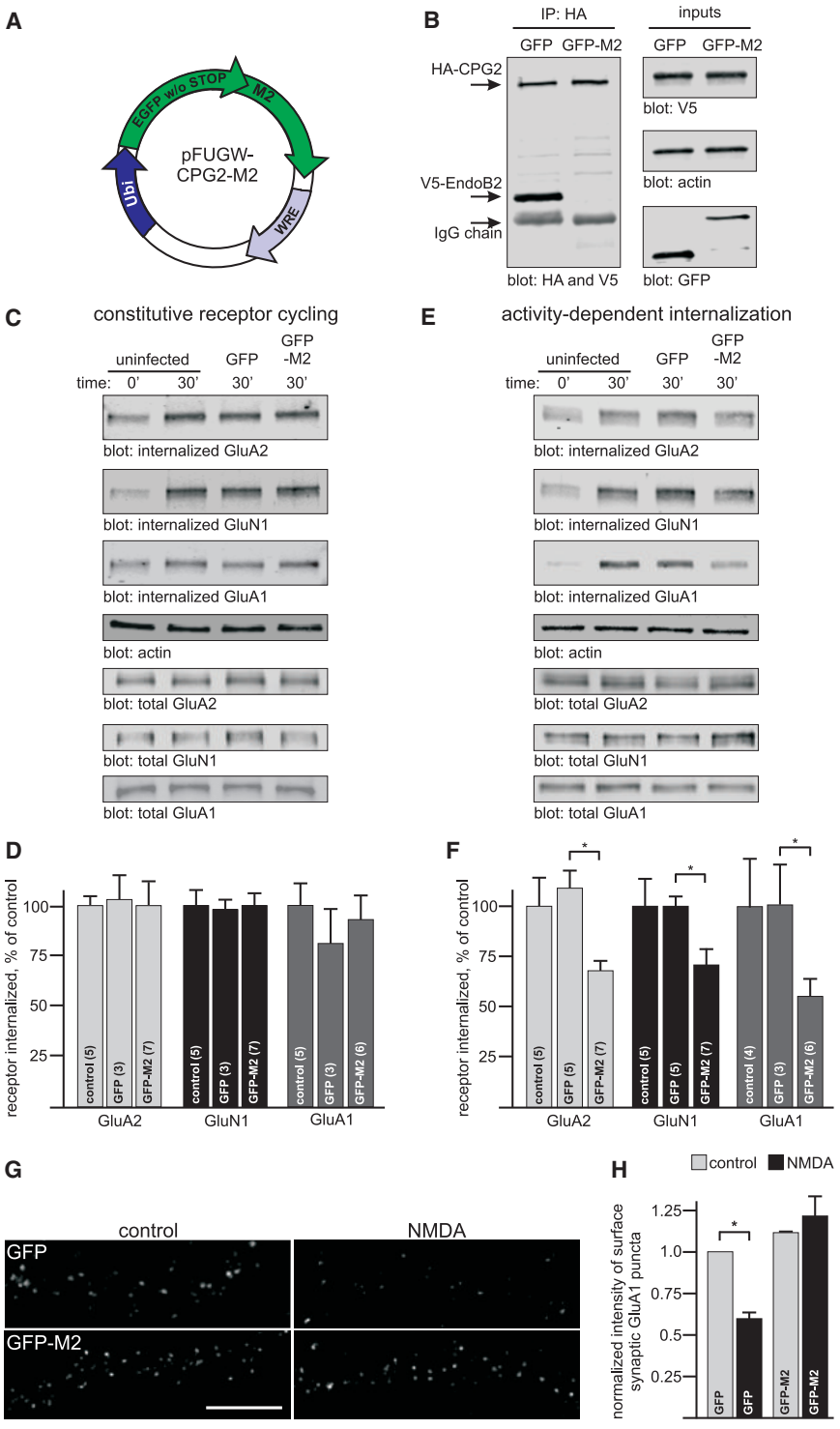

Figure 7. The Interaction of CPG2 with Endophilin B2 Is Critical for Activity-Dependent Glutamate Receptor Internalization

(A) Schematic of the lentiviral vector used to drive expression of either GFP alone or M2 fused to GFP under the control of the ubiquitin promoter (Ubi). WRE, woodchuck regulatory element.

(B) Overexpression of M2 effectively blocks association of endophilin B2 with CPG2. (Left) Co-immunoprecipitations from HEK293T cells that express HA-tagged CPG2, V5-tagged endophilin B2, and either GFP or GFP-M2 is shown. (Right) Blots showing equal input material are shown.

(C) Constitutive cycling of glutamate receptor subunits in cortical cultures that were uninfected or infected with lentivirus expressing either GFP alone or M2 fused to GFP. Surface proteins of cultures, infected as indicated, were labeled at 4°C with a cleavable biotin tag. Surface labels were stripped after 30 min at 37°C, and internalized membrane proteins were affinity purified. Representative western blots for GluA2, GluN1, and GluA1 are shown. Actin levels confirm equal input material. Total GluA2, GluN1, and GluA1 levels are unaffected by viral infection.

(D) Quantification of internalized receptors through constitutive cycling after 30 min represented as percent of control ± SEM: GFP-M2 compared to control: 1.0 ± 0.12 for GluA2, p = 0.99, Student's t test; 1.0 ± 0.06 for GluN1, p = 0.81, Student's t test; 0.93 ± 0.12 for GluA1, p = 0.29, Student's t test; n values indicated in parenthesis for each condition.

(E) Activity-dependent internalization of glutamate receptors in the presence of 100 μM picrotoxin.

(F) Quantification of activity-dependent internalization of glutamate receptors shown as percent of control ± SEM: GFP-M2 relative to control: 0.68 ± 0.05 for GluA2, 0.71 ± 0.08 for GluN1, 0.55 ± 0.09 for GluA1; n values indicated in parenthesis for each condition. *p < 0.05; Student's t test.

(G) Immuno-staining of surface GluA1 in neurons infected with GFP or GFP-M2, under control conditions (left panel) or after NMDA-induced AMPA receptor internalization (right panel). The scale bar represents 15 μm.

(H) Quantification of synaptic GluA1 puncta intensity normalized to control ± SEM: GFP relative to control: 0.52 ± 5.2, n = 3 experiments, 20 cells, 494 puncta for control; 18 cells, 552 puncta for NMDA; *p < 0.05; Student's t test; GFP-M2 relative to control: 1.22 ± 0.12, n = 3 experiments, 14 cells, 324 puncta for control; 19 cells, 372 puncta for NMDA; p = 0.57; Student's t test.

internalized [11, 51] (reviewed in [52, 53]), leading to LTD of postsynaptic responses. NMDARs too get internalized after stimulation, although to a lesser extent [11, 54–57]. Whereas constitutive versus activity-dependent internalization processes are mechanistically distinct in timing and regulation [58, 59], it has not been clear how they are differentially regulated by an apparently ubiquitous endocytic apparatus. The requirement for CPG2 is also ubiquitous to both constitutive and activity-dependent CME and both AMPAR and NMDAR. Yet, the demonstration that EndoB2 is recruited by CPG2 only for activity-dependent CME illustrates how even a general regulator of GluR CME can engage the more-ubiquitous core components of the endocytic machinery via different binding partners—dependent on cellular conditions.

The ability through EndoB2 to specifically disrupt activity-dependent glutamate receptor CME without affecting constitutive receptor cycling reveals another interesting aspect of their relationship. We don't see a direct effect of picrotoxin on GluA2 and GluN1 internalization but see an effect of the M2 dominant negative on their internalization in the presence of picrotoxin (also for the effect of EndoB2 KD). An interesting possibility consistent with these results is that constitutive and activity-dependent internalization of these subunits is not cumulative but rather interchangeable. Addition of picrotoxin converts constitutive to activity dependent. For GluA1, there is potentially an additional activity-dependent mechanism not shared with other subunits.

In summary, we find that, by using a specific intermediate, EndoB2, CPG2 can selectively recruit the endocytic machinery for CME of synaptic glutamate receptors only in response to synaptic activity. This provides a hint as to how the ubiquitous machinery of CME may be specifically engaged by intermediates that act only in a precise cellular context. Cellular context may be implemented by second messenger pathways that are responsive to synaptic activity, such as the PKA pathway that engages CPG2. A rich area of future investigation is how synaptic activity triggers different plasticity mechanisms that are Hebbian, such as LTP and LTD, or homeostatic, such as synaptic scaling up or down, using a finite number of molecular players.

EXPERIMENTAL PROCEDURES

All animal work was approved by the Massachusetts Institute of Technology Committee on Animal Care and meets the NIH guidelines for the use and care of vertebrate animals.

Internalization Assay

Cortical neurons from E18 Sprague-Dawley rat embryos were seeded at 4×10^6 cells per 10-cm dish and incubated in 2% B27 and 1% Glutamax for 15 days. Surface proteins were labeled with a cleavable biotin tag, and internalization of surface receptors was allowed for 30 min at 37°C. Remaining surface labels were stripped with TCEP at pH 7.5 and then with reduced glutathione at pH 8.7. Glutathione was quenched with 5 mg/ml iodocetamide at pH 8.7. Cells were lysed, and biotin-labeled proteins were affinity isolated with Neutravidin-covered agarose beads added to 300 μg of the cleared lysate. Where appropriate, neurons were infected with lentiviral particles to MOI > 90% 4 days prior to the assay to allow genomic insertion and robust expression of GFP, or GFP-M2.

Picrotoxin LTD Protocol

One hundred micromolar picrotoxin (Sigma) was administered to neurons during the 1-hr preincubation with leupeptin (AG Scientific; 100 μg/ml), as well as during the 30-min internalization period. Picrotoxin solution was prepared fresh in ethanol, and vehicle controls were included to rule out solvent effects.

Chemical LTD Assay

Hippocampal neurons from E18 Sprague-Dawley rat embryos were cultured for 21 days on glass coverslips in Neurobasal media with 2% B27 supplement and 1% Glutamax. Neurons were incubated with 2 μM tetrodotoxin for 1 hr and then in 10 μg/ml rabbit anti-GluA1 primary antibody (Calbiochem; PC246) for 15 min at 37°C. Cells were either fixed (surface stain only) or treated in 2 μM tetrodotoxin plus 50 μM NMDA for 4 min at 37°C, returned to the incubator in neuron conditioned media for another 15 min, and then fixed (chemical LTD protocol). Cells were stained with anti-rabbit secondary antibody coupled to Alexa Fluor 546. Pixel intensity of synaptic GluA1 clusters was analyzed using ImageJ software.

F-Actin Binding Assay

F-actin binding was performed essentially as described [8]. In brief, rabbit muscle actin (Sigma) was allowed to polymerize at room temperature after addition of salt and ATP, according to the manufacturer's instructions. CPG2 and EndoB2 were in vitro transcribed and translated using an in vitro transcription and translation (TNT) mix system (Promega) and ^{35}S-labeled methionine (PerkinElmer).

Triton X-100 Extraction

Cultured hippocampal neurons were washed with ice cold PBS and then carefully exposed to ice-cold 0.5% Triton X-100 in PBS (v/v) for 2 min on ice. Cells were fixed immediately with 4% PFA (w/v) containing 4% sucrose (w/v) for 12 min and subsequently prepared for immunocytochemistry as described [8].

Fluorescence Microscopy and Immunocytochemistry Quantification

Images were obtained using a Nikon epifluorescent scope. All images are wide-field fluorescence and obtained with Spot Software. Quantification of immunocytochemistry was conducted using ImageJ software to obtain pixel intensity values in a linear range within regions of interest (ROI). ROIs were positioned over spine heads labeled with rhodamine phalloidin, and the corresponding staining intensity was measured from the green channel labeling either EndoB2 or clathrin heavy chain. ImageJ a.u. of fluorescence intensity for each condition were quantified relative to control arbitrary values averaged from each imaging session.

SUPPLEMENTAL INFORMATION

Supplemental Information includes Supplemental Experimental Procedures and three figures and can be found with this article online at http://dx.doi.org/10.1016/j.cub.2015.11.071.

AUTHOR CONTRIBUTIONS

S.L. and M.R.B. designed and conducted experiments and analyzed data. J.A.K., J.R.C., and J.G. conducted experiments. E.N. designed and supervised the study. S.L., M.R.B., and E.N. wrote the manuscript.

ACKNOWLEDGMENTS

We thank the members of the E.N. lab for critical reading of the manuscript. This work was supported by funding from the Picower Institute Innovation Fund (to E.N.) and scholarship LO 1455/1-1 from the Deutsche Forschungsgemeinschaft (to S.L.).

Received: October 30, 2014
Revised: September 21, 2015
Accepted: November 30, 2015
Published: January 14, 2016

REFERENCES

1. Lee, S.H., Liu, L., Wang, Y.T., and Sheng, M. (2002). Clathrin adaptor AP2 and NSF interact with overlapping sites of GluR2 and play distinct roles in AMPA receptor trafficking and hippocampal LTD. Neuron *36*, 661–674.
2. Qualmann, B., Kessels, M.M., and Kelly, R.B. (2000). Molecular links between endocytosis and the actin cytoskeleton. J. Cell Biol. *150*, F111–F116.
3. Loebrich, S. (2014). The role of F-actin in modulating Clathrin-mediated endocytosis: Lessons from neurons in health and neuropsychiatric disorder. Commun. Integr. Biol. *7*, e28740.
4. Boulant, S., Kural, C., Zeeh, J.C., Ubelmann, F., and Kirchhausen, T. (2011). Actin dynamics counteract membrane tension during clathrin-mediated endocytosis. Nat. Cell Biol. *13*, 1124–1131.
5. Legendre-Guillemin, V., Metzler, M., Charbonneau, M., Gan, L., Chopra, V., Philie, J., Hayden, M.R., and McPherson, P.S. (2002). HIP1 and HIP12 display differential binding to F-actin, AP2, and clathrin.

Identification of a novel interaction with clathrin light chain. J. Biol. Chem. *277*, 19897–19904.

6. Kaksonen, M., Toret, C.P., and Drubin, D.G. (2006). Harnessing actin dynamics for clathrin-mediated endocytosis. Nat. Rev. Mol. Cell Biol. *7*, 404–414.
7. Cottrell, J.R., Borok, E., Horvath, T.L., and Nedivi, E. (2004). CPG2: a brain- and synapse-specific protein that regulates the endocytosis of glutamate receptors. Neuron *44*, 677–690.
8. Loebrich, S., Djukic, B., Tong, Z.J., Cottrell, J.R., Turrigiano, G.G., and Nedivi, E. (2013). Regulation of glutamate receptor internalization by the spine cytoskeleton is mediated by its PKA-dependent association with CPG2. Proc. Natl. Acad. Sci. USA *110*, E4548–E4556.
9. Kjaerulff, O., Brodin, L., and Jung, A. (2011). The structure and function of endophilin proteins. Cell Biochem. Biophys. *60*, 137–154.
10. Fievet, B.T., Gautreau, A., Roy, C., Del Maestro, L., Mangeat, P., Louvard, D., and Arpin, M. (2004). Phosphoinositide binding and phosphorylation act sequentially in the activation mechanism of ezrin. J. Cell Biol. *164*, 653–659.
11. Ehlers, M.D. (2000). Reinsertion or degradation of AMPA receptors determined by activity-dependent endocytic sorting. Neuron *28*, 511–525.
12. Fujimoto, L.M., Roth, R., Heuser, J.E., and Schmid, S.L. (2000). Actin assembly plays a variable, but not obligatory role in receptor-mediated endocytosis in mammalian cells. Traffic *1*, 161–171.
13. Merrifield, C.J., Feldman, M.E., Wan, L., and Almers, W. (2002). Imaging actin and dynamin recruitment during invagination of single clathrin-coated pits. Nat. Cell Biol. *4*, 691–698.
14. Yarar, D., Waterman-Storer, C.M., and Schmid, S.L. (2005). A dynamic actin cytoskeleton functions at multiple stages of clathrin-mediated endocytosis. Mol. Biol. Cell *16*, 964–975.
15. Allison, D.W., Gelfand, V.I., Spector, I., and Craig, A.M. (1998). Role of actin in anchoring postsynaptic receptors in cultured hippocampal neurons: differential attachment of NMDA versus AMPA receptors. J. Neurosci. *18*, 2423–2436.
16. Kim, C.H., and Lisman, J.E. (1999). A role of actin filament in synaptic transmission and long-term potentiation. J. Neurosci. *19*, 4314–4324.
17. Zhou, Q., Xiao, M., and Nicoll, R.A. (2001). Contribution of cytoskeleton to the internalization of AMPA receptors. Proc. Natl. Acad. Sci. USA *98*, 1261–1266.
18. Schulz, T.W., Nakagawa, T., Licznerski, P., Pawlak, V., Kolleker, A., Rozov, A., Kim, J., Dittgen, T., Köhr, G., Sheng, M., et al. (2004). Actin/alpha-actinin-dependent transport of AMPA receptors in dendritic spines: role of the PDZ-LIM protein RIL. J. Neurosci. *24*, 8584–8594.
19. Han, K., Holder, J.L., Jr., Schaaf, C.P., Lu, H., Chen, H., Kang, H., Tang, J., Wu, Z., Hao, S., Cheung, S.W., et al. (2013). SHANK3 overexpression causes manic-like behaviour with unique pharmacogenetic properties. Nature *503*, 72–77.
20. Vannier, C., Pesty, A., San-Roman, M.J., and Schmidt, A.A. (2013). The Bin/amphiphysin/Rvs (BAR) domain protein endophilin B2 interacts with plectin and controls perinuclear cytoskeletal architecture. J. Biol. Chem. *288*, 27619–27637.
21. Witke, W., Podtelejnikov, A.V., Di Nardo, A., Sutherland, J.D., Gurniak, C.B., Dotti, C., and Mann, M. (1998). In mouse brain profilin I and profilin II associate with regulators of the endocytic pathway and actin assembly. EMBO J. *17*, 967–976.
22. McNiven, M.A., Kim, L., Krueger, E.W., Orth, J.D., Cao, H., and Wong, T.W. (2000). Regulated interactions between dynamin and the actin-binding protein cortactin modulate cell shape. J. Cell Biol. *151*, 187–198.
23. Kessels, M.M., Engqvist-Goldstein, A.E., Drubin, D.G., and Qualmann, B. (2001). Mammalian Abp1, a signal-responsive F-actin-binding protein, links the actin cytoskeleton to endocytosis via the GTPase dynamin. J. Cell Biol. *153*, 351–366.
24. Shin, N., Lee, S., Ahn, N., Kim, S.A., Ahn, S.G., YongPark, Z., and Chang, S. (2007). Sorting nexin 9 interacts with dynamin 1 and N-WASP and coordinates synaptic vesicle endocytosis. J. Biol. Chem. *282*, 28939–28950.
25. Humphries, A.C., Donnelly, S.K., and Way, M. (2014). Cdc42 and the Rho GEF intersectin-1 collaborate with Nck to promote N-WASP-dependent actin polymerisation. J. Cell Sci. *127*, 673–685.
26. Waelter, S., Scherzinger, E., Hasenbank, R., Nordhoff, E., Lurz, R., Goehler, H., Gauss, C., Sathasivam, K., Bates, G.P., Lehrach, H., and Wanker, E.E. (2001). The huntingtin interacting protein HIP1 is a clathrin and alpha-adaptin-binding protein involved in receptor-mediated endocytosis. Hum. Mol. Genet. *10*, 1807–1817.
27. Metzler, M., Li, B., Gan, L., Georgiou, J., Gutekunst, C.A., Wang, Y., Torre, E., Devon, R.S., Oh, R., Legendre-Guillemin, V., et al. (2003). Disruption of the endocytic protein HIP1 results in neurological deficits and decreased AMPA receptor trafficking. EMBO J. *22*, 3254–3266.
28. Chowdhury, S., Shepherd, J.D., Okuno, H., Lyford, G., Petralia, R.S., Plath, N., Kuhl, D., Huganir, R.L., and Worley, P.F. (2006). Arc/Arg3.1 interacts with the endocytic machinery to regulate AMPA receptor trafficking. Neuron *52*, 445–459.
29. Lyford, G.L., Yamagata, K., Kaufmann, W.E., Barnes, C.A., Sanders, L.K., Copeland, N.G., Gilbert, D.J., Jenkins, N.A., Lanahan, A.A., and Worley, P.F. (1995). Arc, a growth factor and activity-regulated gene, encodes a novel cytoskeleton-associated protein that is enriched in neuronal dendrites. Neuron *14*, 433–445.
30. Guzowski, J.F., Lyford, G.L., Stevenson, G.D., Houston, F.P., McGaugh, J.L., Worley, P.F., and Barnes, C.A. (2000). Inhibition of activity-dependent arc protein expression in the rat hippocampus impairs the maintenance of long-term potentiation and the consolidation of long-term memory. J. Neurosci. *20*, 3993–4001.
31. Messaoudi, E., Kanhema, T., Soulé, J., Tiron, A., Dagyte, G., da Silva, B., and Bramham, C.R. (2007). Sustained Arc/Arg3.1 synthesis controls long-term potentiation consolidation through regulation of local actin polymerization in the dentate gyrus in vivo. J. Neurosci. *27*, 10445–10455.
32. Bai, J., Hu, Z., Dittman, J.S., Pym, E.C., and Kaplan, J.M. (2010). Endophilin functions as a membrane-bending molecule and is delivered to endocytic zones by exocytosis. Cell *143*, 430–441.
33. Gallop, J.L., Jao, C.C., Kent, H.M., Butler, P.J.G., Evans, P.R., Langen, R., and McMahon, H.T. (2006). Mechanism of endophilin N-BAR domain-mediated membrane curvature. EMBO J. *25*, 2898–2910.
34. Mim, C., Cui, H., Gawronski-Salerno, J.A., Frost, A., Lyman, E., Voth, G.A., and Unger, V.M. (2012). Structural basis of membrane bending by the N-BAR protein endophilin. Cell *149*, 137–145.
35. Sundborger, A., Soderblom, C., Vorontsova, O., Evergren, E., Hinshaw, J.E., and Shupliakov, O. (2011). An endophilin-dynamin complex promotes budding of clathrin-coated vesicles during synaptic vesicle recycling. J. Cell Sci. *124*, 133–143.
36. Verstreken, P., Koh, T.-W., Schulze, K.L., Zhai, R.G., Hiesinger, P.R., Zhou, Y., Mehta, S.Q., Cao, Y., Roos, J., and Bellen, H.J. (2003). Synaptojanin is recruited by endophilin to promote synaptic vesicle uncoating. Neuron *40*, 733–748.
37. Schuske, K.R., Richmond, J.E., Matthies, D.S., Davis, W.S., Runz, S., Rube, D.A., van der Bliek, A.M., and Jorgensen, E.M. (2003). Endophilin is required for synaptic vesicle endocytosis by localizing synaptojanin. Neuron *40*, 749–762.
38. Renard, H.-F., Simunovic, M., Lemière, J., Boucrot, E., Garcia-Castillo, M.D., Arumugam, S., Chambon, V., Lamaze, C., Wunder, C., Kenworthy, A.K., et al. (2015). Endophilin-A2 functions in membrane scission in clathrin-independent endocytosis. Nature *517*, 493–496.
39. Boucrot, E., Ferreira, A.P., Almeida-Souza, L., Debard, S., Vallis, Y., Howard, G., Bertot, L., Sauvonnet, N., and McMahon, H.T. (2015). Endophilin marks and controls a clathrin-independent endocytic pathway. Nature *517*, 460–465.
40. Cremona, O., Di Paolo, G., Wenk, M.R., Lüthi, A., Kim, W.T., Takei, K., Daniell, L., Nemoto, Y., Shears, S.B., Flavell, R.A., et al. (1999). Essential role of phosphoinositide metabolism in synaptic vesicle recycling. Cell *99*, 179–188.

 ©2016 Elsevier Ltd All rights reserved

41. Waung, M.W., Pfeiffer, B.E., Nosyreva, E.D., Ronesi, J.A., and Huber, K.M. (2008). Rapid translation of Arc/Arg3.1 selectively mediates mGluR-dependent LTD through persistent increases in AMPAR endocytosis rate. Neuron *59*, 84–97.

42. Park, S., Park, J.M., Kim, S., Kim, J.-A., Shepherd, J.D., Smith-Hicks, C.L., Chowdhury, S., Kaufmann, W., Kuhl, D., Ryazanov, A.G., et al. (2008). Elongation factor 2 and fragile X mental retardation protein control the dynamic translation of Arc/Arg3.1 essential for mGluR-LTD. Neuron *59*, 70–83.

43. Jakkamsetti, V., Tsai, N.-P., Gross, C., Molinaro, G., Collins, K.A., Nicoletti, F., Wang, K.H., Osten, P., Bassell, G.J., Gibson, J.R., and Huber, K.M. (2013). Experience-induced Arc/Arg3.1 primes CA1 pyramidal neurons for metabotropic glutamate receptor-dependent long-term synaptic depression. Neuron *80*, 72–79.

44. Plath, N., Ohana, O., Dammermann, B., Errington, M.L., Schmitz, D., Gross, C., Mao, X., Engelsberg, A., Mahlke, C., Welzl, H., et al. (2006). Arc/Arg3.1 is essential for the consolidation of synaptic plasticity and memories. Neuron *52*, 437–444.

45. Rial Verde, E.M., Lee-Osbourne, J., Worley, P.F., Malinow, R., and Cline, H.T. (2006). Increased expression of the immediate-early gene arc/arg3.1 reduces AMPA receptor-mediated synaptic transmission. Neuron *52*, 461–474.

46. Papa, M., and Segal, M. (1996). Morphological plasticity in dendritic spines of cultured hippocampal neurons. Neuroscience *71*, 1005–1011.

47. Otmakhov, N., Tao-Cheng, J.-H., Carpenter, S., Asrican, B., Dosemeci, A., Reese, T.S., and Lisman, J. (2004). Persistent accumulation of calcium/calmodulin-dependent protein kinase II in dendritic spines after induction of NMDA receptor-dependent chemical long-term potentiation. J. Neurosci. *24*, 9324–9331.

48. Molnár, E. (2011). Long-term potentiation in cultured hippocampal neurons. Semin. Cell Dev. Biol. *22*, 506–513.

49. Lüscher, C., Xia, H., Beattie, E.C., Carroll, R.C., von Zastrow, M., Malenka, R.C., and Nicoll, R.A. (1999). Role of AMPA receptor cycling in synaptic transmission and plasticity. Neuron *24*, 649–658.

50. Maher, B.J., Mackinnon, R.L., 2nd, Bai, J., Chapman, E.R., and Kelly, P.T. (2005). Activation of postsynaptic Ca(2+) stores modulates glutamate receptor cycling in hippocampal neurons. J. Neurophysiol. *93*, 178–188.

51. Casimiro, T.M., Nawy, S., and Carroll, R.C. (2013). Molecular mechanisms underlying activity-dependent AMPA receptor cycling in retinal ganglion cells. Mol. Cell. Neurosci. *56*, 384–392.

52. Carroll, R.C., Beattie, E.C., von Zastrow, M., and Malenka, R.C. (2001). Role of AMPA receptor endocytosis in synaptic plasticity. Nat. Rev. Neurosci. *2*, 315–324.

53. Shepherd, J.D., and Huganir, R.L. (2007). The cell biology of synaptic plasticity: AMPA receptor trafficking. Annu. Rev. Cell Dev. Biol. *23*, 613–643.

54. Han, L., Campanucci, V.A., Cooke, J., and Salter, M.W. (2013). Identification of a single amino acid in GluN1 that is critical for glycine-primed internalization of NMDA receptors. Mol. Brain *6*, 36.

55. Snyder, E.M., Philpot, B.D., Huber, K.M., Dong, X., Fallon, J.R., and Bear, M.F. (2001). Internalization of ionotropic glutamate receptors in response to mGluR activation. Nat. Neurosci. *4*, 1079–1085.

56. Nong, Y., Huang, Y.-Q., Ju, W., Kalia, L.V., Ahmadian, G., Wang, Y.T., and Salter, M.W. (2003). Glycine binding primes NMDA receptor internalization. Nature *422*, 302–307.

57. Roche, K.W., Standley, S., McCallum, J., Dune Ly, C., Ehlers, M.D., and Wenthold, R.J. (2001). Molecular determinants of NMDA receptor internalization. Nat. Neurosci. *4*, 794–802.

58. Lin, J.W., Ju, W., Foster, K., Lee, S.H., Ahmadian, G., Wyszynski, M., Wang, Y.T., and Sheng, M. (2000). Distinct molecular mechanisms and divergent endocytotic pathways of AMPA receptor internalization. Nat. Neurosci. *3*, 1282–1290.

59. Brown, T.C., Tran, I.C., Backos, D.S., and Esteban, J.A. (2005). NMDA receptor-dependent activation of the small GTPase Rab5 drives the removal of synaptic AMPA receptors during hippocampal LTD. Neuron *45*, 81–94.